Volume 16 Number 20 1988 Nucleic Acids Research

Empirical estimation of protein-induced DNA bending angles: applications to λ site-specific recombination complexes

John F.Thompson+ and Arthur Landy*

Division of Biology and Medicine, Brown University, Providence, RI 02912, USA

Received June 9, 1988; Revised and Accepted September 15, 1988

ABSTRACT

Protein-induced DNA bending is an important element in the structure of many protein-DNA complexes, including those involved in replication, transcription, and recombination. To understand these structures, the path followed by the DNA in each complex must be established. We have generated an empirical relation between the degree of bending and the altered electrophoretic mobility in polyacrylamide gels that allows estimation of protein-induced bends. This technique has been used to analyze 17 different protein-DNA complexes formed by six proteins including the four proteins involved in lambda site-specific recombination. The simplicity of this technique should make it useful in estimating angles for the construction of models of protein-DNA complexes and readily applicable to many systems where questions of higher-order structure are important for understanding function.

INTRODUCTION

Complex protein-DNA structures are responsible for both the storage and expression of genetic information. Unraveling the manner in which these components interact to execute specific cellular processes has been the object of considerable study. Examples of higher order complexes involving multiple proteins and hundreds of base pairs of DNA include those responsible for enhancing transcription, effecting site-specific recombination, and initiating DNA replication (reviewed in 1,2). Analysis of such structures has been attempted at two levels: gross structure has been visualized by electron microscopy and detailed structure has been probed chemically and enzymatically. To obtain a functional understanding of these complexes, it is necessary to bridge the gap between these levels. The system in which the most detailed structural information has been obtained is that of the nucleosome in which 140 bp of DNA is wrapped relatively

smoothly around a histone core (3,4). One of the invaluable features of this model has been to establish the flexibility of DNA when interacting with proteins. In contrast to nucleosomes, other complexes involving highly specific interactions may result in very different types of structures.

One interesting set of complexes that has been extensively analyzed and displays a high degree of specificity and cooperativity is that necessary for the site-specific recombination reactions in bacteriophage lambda (reviewed in 5,6). In addition to executing a precise and efficient rearrangement of DNA sequences, these complexes are able to incorporate features that make the reactions unidirectional in a manner that is tightly coupled to the concentration of the phage and host proteins involved (7-9). These proteins, the virally-encoded Int and Xis and the bacterially-encoded IHF and FIS, interact with 240 bp of phage DNA and 30 bp of bacterial DNA to carry out integration and excision. Efforts to characterize the structure of these complexes have included nuclease protection and chemical modification studies with proteins bound to wild-type and mutated DNA (7-17). These studies have yielded the linear arrays of protein binding sites required for the reactions (Fig. 1A) but have led to only limited insight into the three-dimensional structure of the recombinogenic complexes. To begin assembling these arrays in three dimensions, we have characterized each of the proteins involved in the reactions for its ability to bend DNA.

Bent or curved DNA has been detected in a number of contexts including the relatively smooth bending of DNA around the nucleosome core and the stable intrinsic curvature observed in kinetoplast DNA. Intrinsically curved DNA was originally identified on the basis of its anomalous electrophoretic mobility (18). Other physical techniques have confirmed that this results from a stable curvature in solution (18-25) with the sequences responsible shown to be blocks of more than two adjacent adenine residues that are present in phase with the helical repeat (18,26-28). Both natural DNA and synthetic oligomers with this type of sequence have been extensively studied (18-29).

The altered electrophoretic mobility of intrinsically curved

DNA has been attributed to the reduction in the end-to-end distance of the polymer (26,30). The aberrant mobility of A tract-containing oligomers has been used to characterize the detailed nature of the bends (29) while longer fragments have been used to identify proteins that bend DNA and to map their locus of bending (26). For a set of DNA fragments with the same length, the end-to-end distance will depend on where the bend-inducing protein is bound on the fragment. Only some DNA binding

Table I: Plasmids for Generating Permuted Restriction Fragments

Plasmid	Parent	Duplication Boundaries		Duplication Length (bp)	Binding Sites
JT81	JT14	AhaII(4286)	NarI(413)	300	H1 P1 RI
JT82	JT41	AhaII(4286)	NarI(413)	298	P1 RI
JT110		reference 48		371	X1 X2 F H2
JT117	JT58	AhaII(4286)	NarI(413)	344	H′ P′123
JT118	JT58	AhaII(3904)	NarI(413)	726	H′ P′123
JT143	BF504	BglII	NaeI(769)	440	C C′
JT145	UC13	NarI	PvuII(622)	387	lac

Table I legend: The construction of plasmids with duplicated protein binding sites is shown (see also Fig. 1). Plasmids pJT14, pJT41 (8), pJT95, pJT110 (48), pSN1, pSN2 (40), and pUC13 (49) have been described. To make duplications for permutation analysis, plasmids with appropriately situated protein binding sites were subjected to two pairwise digestions. In each case, one cleavage site was in or near the ampicillin gene (using PstI or Eco0109). The other cleavage was to the right or left of the region of interest using the enzymes listed under "duplication boundaries"; coordinates are given in parenthesis for enzymes with multiple sites. The listed coordinates are for unaltered pUC13 and pBR322 backbones. The fragments from each pairwise digestion containing the binding sites were gel purified and ligated together; and, when necessary, the overhangs adjacent to the duplicated region were filled in with DNA polymerase (large fragment). This procedure regenerates the entire plasmid backbone and duplicates the region of interest in direct repeat. In addition to using duplicated regions, entire plasmids can also be used to generate permuted sequences of full plasmid length as was done with both pJT58 and pJT130. pJT58 was made by cutting pSN1 at both EcoRI sites and religating (thus deleting the DNA between the pBR322 EcoRI site and the EcoRI site between the C′ and H′ binding sites). pJT130 was made from pJT58 by digesting with NaeI and religating, deleting the 882 bp between the outer sites. pBF504 contains a wild-type core sequence made synthetically with linkers on either end and inserted between the HindIII and BamHI sites of pBR327 (B. Franz, unpublished results).

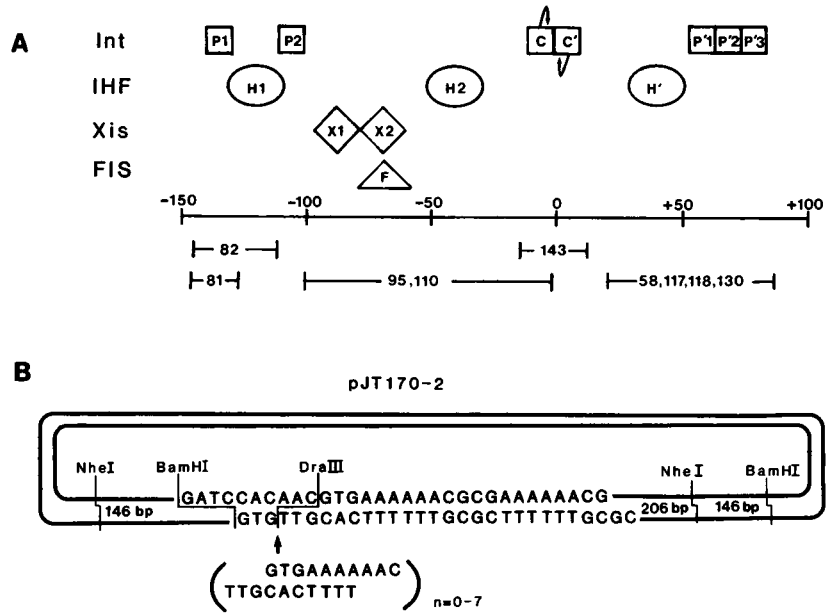

Fig. 1. A) Protein binding sites in attP. Coordinates for the 250 bp attP site extend from -150 to +100 (horizontal axis). Below the coordinate axis are numbers corresponding to the plasmids listed in Tables I and II; the brackets indicate the protein binding sites present as part of a direct repeat in that plasmid. The integration reaction, in which supercoiled attP DNA recombines with linear attB DNA, requires two proteins: the phage-encoded Int and the host-encoded IHF (50,51). Int binds to two distinct recognition sequences. In both attP and attB, there are two core-type Int binding sites (boxes with arrow) flanking the points of strand exchange (10). In addition, there are five arm-type Int binding sites (boxes) distal to the core region on attP (11). IHF is an accessory protein that binds to three sites (circles) on attP (12). The excision reaction, in which attL and attR recombine to regenerate attP and attB, requires the same two proteins as well as the phage-encoded Xis (52). Xis binds cooperatively to two sites (diamonds) on attP and attR and also inhibits the integration reaction (13,52). In addition, the host-encoded FIS (triangle) modulates the excision reaction by replacing Xis at the X2 site and lowering the concentration of Xis required for the reaction (17).
B) Construction of plasmids with multiple A tracts. The sequence of the two A tracts in the plasmid pJT170-2 is shown. This plasmid was made by inserting the 29mer and 31mer shown into pBR327 as a single copy separating a directly repeated region (from the ClaI site to the BamHI site) using the strategy described in Table I. The oligomer sequence was such that the BamHI site was regenerated and the ClaI site adjacent to the A tract was destroyed. Because the A tracts are between duplicated regions, they need only be present in one copy to obtain

circularly permuted fragments (53). Additional A tracts with the sequence shown were inserted into the single DraIII site present in pJT170-2 to generate plasmids pJT170-3 through pJT170-9 (for n=1 to 7). The correct polarity and phasing were maintained because of the asymmetric overhang generated by DraIII. Each insert regenerated the DraIII site at the left end and destroyed it at the right end.

proteins induce bending and the degree of bending is likely to be a characteristic of each individual protein. The magnitude of the bends induced by various proteins clearly could have important consequences for the overall structure of any protein-DNA complex. The behavior of the four proteins relevant to lambda recombination (Int, IHF, Xis and FIS) has been studied and compared with other examples of DNA bending. The resultant estimates of bending angles make it possible to initiate model building of the protein-DNA complexes involved in recombination.

MATERIALS AND METHODS

Int, IHF, and Xis were purified as described (9). FIS and CAP were generous gifts from R. Kahmann and D. Crothers, respectively. All other proteins were obtained from New England Biolabs. Construction of plasmids is described in Table I and Figure 1. DNA fragments for mobility shift analysis were labeled with T_4 DNA polymerase and [α-^{32}P] dATP, purified on 2% agarose gels, and eluted from the gels with Geneclean as described by Bio 101 (La Jolla, CA). Protein binding was carried out in 20 μl with 100 mM NaCl, 10 mM Tris-HCl (pH 7.5), 1 mM EDTA, 7 mM 2-mercaptoethanol, 1 mg/ml bovine serum albumin and 10 μg/ml salmon sperm DNA. After incubation at room temperature for 15 minutes, Ficoll was added to 1% and the samples loaded on polyacrylamide gels with the voltage applied. Polyacrylamide gels (20 x 20 x 0.1 cm) contained 4-10% acrylamide (30:1, monomer to bis), 45 mM Tris-borate (pH 8.3) and 2.5 mM EDTA and were run at 10 V/cm at room temperature. Gels were pre-run for 1-3 hours prior to sample loading. Varying the voltage gradient between 2 and 15 V/cm had no effect on the results with DNAs of the lengths used here. After electrophoresis, the gels were dried and autoradiographed.

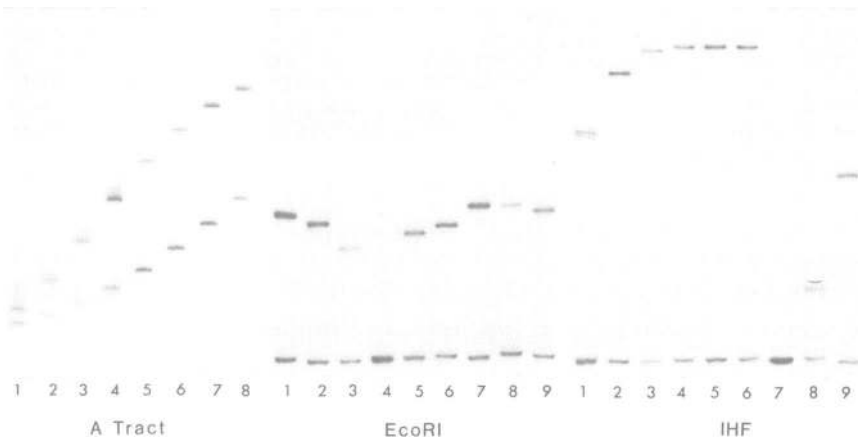

Fig. 2. Mobility shifts of DNA with intrinsic curvature or bound protein. DNA with two to nine A tracts (lanes 1-8 respectively) at the end or the middle of the fragment were obtained by digestion of the plasmids described in Fig. 1B with BamHI or NheI. The faster migrating DNA contains A tracts at the end of the fragment and the slower migrating DNA contains A tracts in the middle of the fragment.

The set of circularly permuted fragments bound to either EcoRI or IHF were obtained by digestion of pJT82 with AhaII, BspHI, Eco0109, EcoRI, ClaI, HindIII, HinfI, Sau3A, or NaeI (lanes 1 to 9, respectively). When the permuted DNA is cleaved within the binding site, no bound fragment is observed for either EcoRI (lane 4) or IHF (lane 7).

RESULTS

Permutation analysis

A DNA sequence containing both an EcoRI and an IHF binding site was used to determine mobility shifts induced by each protein binding to the same set of circularly permuted restriction fragments using the methods described by Wu and Crothers (26) (Fig. 2). Sets of permuted fragments are generated by duplicating a region of DNA containing the binding site(s) of interest followed by cleavage with a restriction enzyme that cuts once in each repeat. This results in fragments with the same length but with the sequence and binding sites positioned differently with respect to the ends of the fragment. Both EcoRI and IHF bind to a single site on the fragments used in Fig. 2 and induce a bend in the DNA as evidenced by the position-dependent alteration in the mobility of DNA fragments with bound protein.

EcoRI binds but does not cleave DNA in the absence of magnesium. As observed with other proteins (26), the DNA with the highest mobility has a protein bound near the end of the fragment and the DNA with the lowest mobility has a protein bound at the middle of the fragment. Identifying the fragments with the highest and lowest mobilities thus allows mapping of the center of bending.

The usefulness of the kind of data shown in Fig. 2 for determining the locus of protein-induced bending has been established in several systems. However, there is clearly more information present than simply the locus of bending. For example, the difference in mobility shift between end-bound and middle-bound EcoRI fragments is small compared to the difference between end-bound and middle-bound IHF fragments. That this difference is related to the degree of bending is evidenced by the behavior of a series of fragments with a variable amount of intrinsic curvature caused by different numbers of A_6 tracts (Fig. 2). As observed previously, the mobility of fragments with phased A tracts at the middle of the fragment is less than that with the A tracts at the end of the fragment (26, Fig. 2) and this difference grows progressively larger with more A tracts (c.f. Fig. 2, lane 1 with two A tracts and lane 8 with nine A tracts).

Relation between curvature and mobility

The lengths of DNA fragments of unknown size are routinely determined by comparison with a series of independently characterized standards (31,32). In an analogous manner, we have used a set of DNAs with independently determined bending angles to relate mobility with degree of bending for use in estimating unknown protein-induced bends.

Because the intrinsically curved A tract DNA has been so extensively studied, we have chosen DNA containing these sequences as standards. The angle of curvature for a single block of three or more adenines quantitated using electric dichroism is 17-19^{o} (21); and, using cyclization kinetics, ranges of 20-22^{o} (24) and 17-22.5^{o} (as cited in 29) have been obtained. Based on these data as well as the crystallographic structure of an A tract oligomer (25), we have used 18^{o} as the angle for each A tract. Improvements in physical techniques may lead to

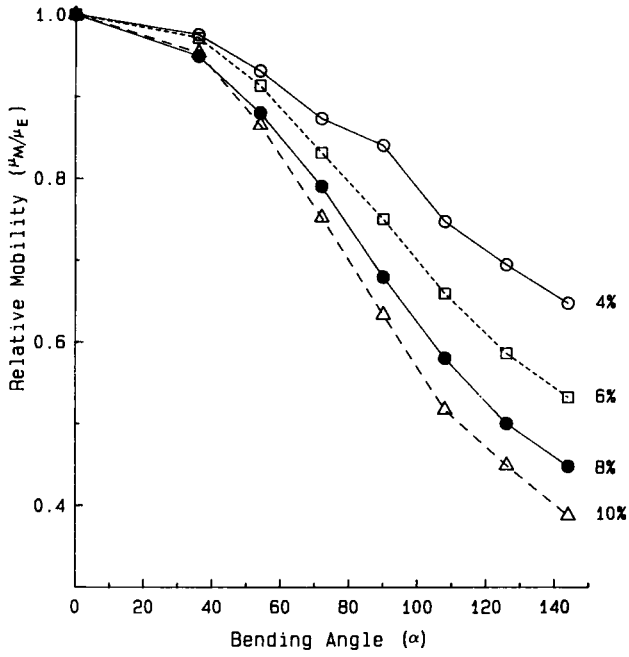

Fig. 3. Relative electrophoretic mobility of A tract DNA at different acrylamide concentrations. The ratio of electrophoretic mobilities of DNAs containing A tracts in the middle versus the end of the fragment is plotted as a function of the predicted bending angle, using 18° per A tract (see text). Gels contained 4% (open circle), 6% (square), 8% (filled circle), or 10% (triangle) acrylamide with electrophoresis and labeling as in Fig. 2.

refinements of this estimate, but the good agreement among three independent techniques suggests this number is reasonable. If a better estimate is forthcoming, it could be used to improve the estimates for protein-induced bending.

The oligomer used for crystallographic analysis contained a tract of six adenines (25) and this length also resulted in the maximum anomalous electrophoretic mobility (28). For tracts of five adenines, optimal phasing (as measured by electrophoretic retardation) is obtained with a helical repeat of ten base pairs (28,29). Based on these results, we have constructed plasmids with different numbers of tandem A_6 tracts and a repeat of ten base pairs (Fig. 1B). Using permuted restriction fragments from these plasmids, relative electrophoretic mobilities were measured

at various acrylamide concentrations and plotted as a function of bending angle (Fig. 3).

While the A tract curvature for fragments with a small number of inserts is likely to be a good model for protein-induced bends, fragments with a large number of inserts should grow progressively less realistic because the curvature becomes delocalized over a region much larger than a typical protein binding site. There are additional uncertainties in equating intrinsic curvature and protein-induced bending including the size of the protein, the detailed structure of the bend, and the dynamics of the complexes. However, these properties are likely to vary significantly even among different protein-DNA complexes so cannot be incorporated into the this type of analysis. Fragments with large numbers of A tracts are also problematic because perfect phasing between repeats cannot be maintained both because ten base pairs is not the exact helical repeat and because the DNA has dynamic motions. The large variation in mobilities observed when fragments with many A tracts are examined at different salt concentrations and temperatures (27) may arise from both these factors. Fragments with short A tracts (like those examined here) are not as subject to variation at low temperature or with magnesium. The delocalization of curvature also introduces error because the DNA cannot be cleaved at the precise center of curvature to obtain the true unbent mobility. This can be corrected by using DNA standards to see where a fragment without a bend should run.

Protein-Induced Bends by Interpolation

The gel mobility shifts induced by various proteins binding to sets of circularly permuted restriction fragments were analyzed for 17 different protein-DNA complexes. For each, the complex with the highest mobility, μ_E, resulted from the fragment with the protein bound nearest the end and the complex with the lowest mobility, μ_M, resulted from the fragment with the protein bound nearest the middle (Fig. 4). For fragments that contain no intrinsic curvature, the ratio of these two mobilities at any of the acrylamide concentrations tested can be used to estimate the bending angle by linear interpolation between points obtained from A tract DNA (Fig. 3). A bending angle of 50 ± 2^{o} is observed

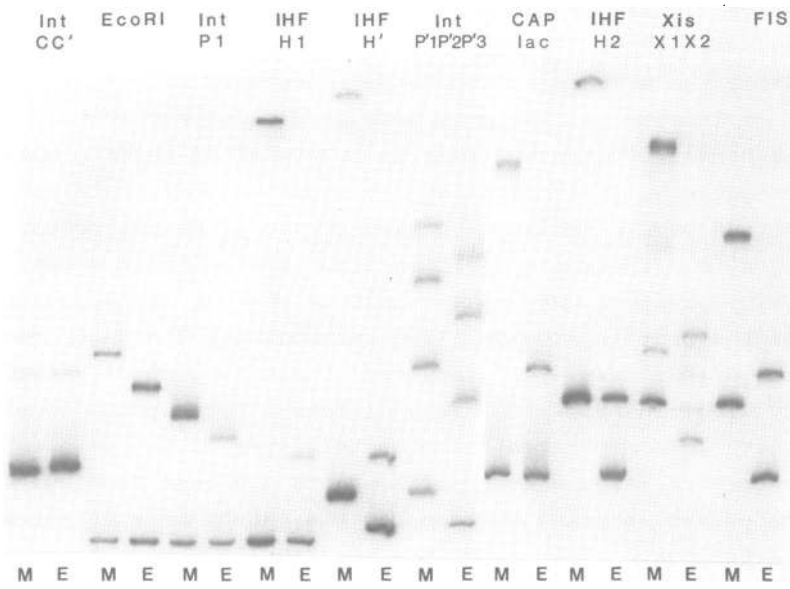

Fig. 4. Mobility shifts induced by end-bound and middle-bound proteins. The protein-bound fragments with the highest (end-bound, E) and lowest (middle-bound, M) electrophoretic mobility are shown for the indicated proteins and binding sites. The enzymes used for digestion and the amounts of protein in each binding reaction are listed in Table II. Electrophoresis in 8% acrylamide was as in Fig. 2. Binding was carried out as in Fig. 2 except 20 μM cyclic AMP was added to both the binding buffer and gels in which CAP was included (26,54).

for EcoRI binding to one set of fragments when measured from 4 to 10% acrylamide. Int binding to the P1 site yields an angle of 38 ± 6^{o} in the same conditions.

For reproducible angles, the protein-bound DNA must be approximately the same length as the standards. If the DNA is too long, the dynamic bending of the DNA becomes significant and reduces the apparent extent of the protein-induced bending. The apparent bending angles for IHF and EcoRI are unchanged when 344 bp fragments are compared with 726 bp fragments while progressively smaller angles are obtained with 2300 and 3100 bp fragments (data not shown). With very short fragments, the length of the bend is large relative to the length of the fragment and is not well-approximated by the standards. For

these reasons, we have used DNA of 300-500 bp for our studies.

For many of the protein binding sites of interest to us, the adjacent DNA contains significant intrinsic curvature as evidenced by the aberrant mobilities of the protein-free fragments. This curvature does not generally coincide with the induced bend and the induced bend could also affect the magnitude or position of the intrinsic curvature so the two are not easily deconvoluted. Ideally, the two effects could be separated by subcloning, but this is not always feasible because of the proximity of A tracts and protein binding sites. Therefore, to obtain the relative mobilities for estimating bends, the ratio of the mobility of the bound to the unbound DNA with the binding site in the middle of the fragment was divided by the same ratio for the DNA with the binding site at the end of the fragment. The inaccuracy introduced by this method of canceling out the contribution of intrinsic curvature should only be significant when it is large in relation to the induced bend.

The bending angles induced by some proteins cannot be estimated by interpolation because they retard the DNA by more than the A tract fragments used as standards. CAP, which is one of these proteins, has been analyzed via crystallography. The structure of CAP has been solved in the absence of DNA and the B-DNA structure has been fit to the protein electrostatic potential (33), leading to a predicted bend of 135-150°. IHF retards the DNA to an even greater extent, suggestive of an even larger bend.

Fitting of A tract mobility to an empirical equation

To facilitate the analysis of the mobility data and the incorporation of CAP as a standard, an empirical equation has been superimposed on the data in Fig. 3 in a manner similar to the fitting of the mobility of unbent DNA to the inverse of its length (31). The mobility of a DNA fragment is related to its end-to-end distance (30); and, for a rigid DNA of contour length L with a bend exactly in the middle of the fragment, this distance can be shown to be L cos $\alpha/2$, with α defined as the angle at which the DNA is bent from linearity. The end-to-end distance of a fragment with the bend at an end will be virtually unchanged and equal to its contour length (L).

When the relative electrophoretic mobilities (μ_M/μ_E) for the

Table II: Protein-Induced Bending Angles

Protein	Binding Site (amt. protein used)	Bending Angles by: Interpolation 4%	5%	6%	7%	8%	10%	mean	Equation
IHF	H1 (1/8u)	-	-	-	-	-	-	-	>140
	H2 (1/16u)	-	-	-	-	-	-	-	>140
	H' (1/16u)	-	-	-	-	-	-	-	>140
Int	P1 (1/8u)	26	39	43	39	39	42	$38^{\pm}6$	40
	P'1 (1/8u)	38	41	37	33	33	40	$36^{\pm}4$	33
	P'1P'2 (1/8u)	45	47	48	45	42	51	$46^{\pm}3$	44
	P'1P'2P'3 (1/8u)	49	53	55	46	48	56	$51^{\pm}4$	49
	CC' (1u)	12	21	17	11	18	21	$17^{\pm}4$	17
Xis	X1X2 (1u)	-	-	-	-	-	-	-	140
	X1 (1u)	44	47	48	45	42	40	$44^{\pm}3$	44
	X2 (1u)	87	91	96	94	93	90	$92^{\pm}3$	97
FIS	F (1/4u)	86	90	95	94	91	85	$90^{\pm}4$	95
Xis FIS	X1F (1/2u;1/8u)	-	-	-	-	-	-	-	>140
CAP	lac (.005 μg)	-	-	-	-	-	-	-	140
EcoRI	AAXTC (5u)	54	48	49	50	50	51	$50^{\pm}2$	52
	GTXAT (5u)	-	-	-	-	-	-	-	66
	TGXTA (5u)	46	52	59	-	60	63	$56^{\pm}6$	63

Table II legend: Binding of proteins to restriction fragments and electrophoresis in acrylamide gels were performed as described in Fig. 2. The amount of protein used is in parenthesis next to each binding site. Bending angles were determined by interpolation at each acrylamide concentration or calculated using data from 8% acrylamide with the equation: $\mu_M/\mu_E=\cos \alpha/2$ (see text and Fig. 5). The mean bending angle from these acrylamide concentrations is shown plus or minus one standard deviation. Intrinsic curvature was corrected for as described in the text. Interpolation was not used for proteins bending by more than 100° (see text). A complete analysis of permuted fragments for each protein binding to the appropriate DNAs was carried out to determine maximum and minimum mobilities. This data was also used to determine the locus of bending for assigning binding site occupancy when more than one binding site for a given protein was present on a fragment. For EcoRI, the recognition site (GAATTC) is denoted as X with the adjacent bases

indicated. Plasmids used to generate fragments for each binding site are listed below (along with the restriction enzymes leading to fragments with the highest and lowest mobility, respectively). pJT81: GTXAT (Sau3A/ClaI); pJT82: H1 and P1 (ClaI/Sau3A), AAXTC (Sau3A/ClaI); pJT110: X1, X2, and X1X2 (SalI/FokI), H2, F, and X1F (SalI/XhoI); pJT117: H', P'1, P'1P'2, and P'1P'2P'3 (HinfI/EcoRI); TGXTA (HinfI/Eco0109); pJT143: CC' (SphI/EcoRI); pJT145: lac (EaeI/BanI).

A-tract fragments in Fig. 3 are fit to equations containing cosine functions, good agreement is found when data from gels containing 8% acrylamide are used in the relation obtained by taking the ratio of the end-to-end distances: $\mu_M/\mu_E=\cos \alpha/2$ (Fig. 5). In these conditions, reasonable predictions are made for the curvature of A tract DNAs containing up to seven inserts and for the bend induced by CAP (Table II). Since this empirical treatment does not address many of the variables that affect electrophoretic mobility, the good agreement indicates that they must be fortuitously canceling out under these conditions of

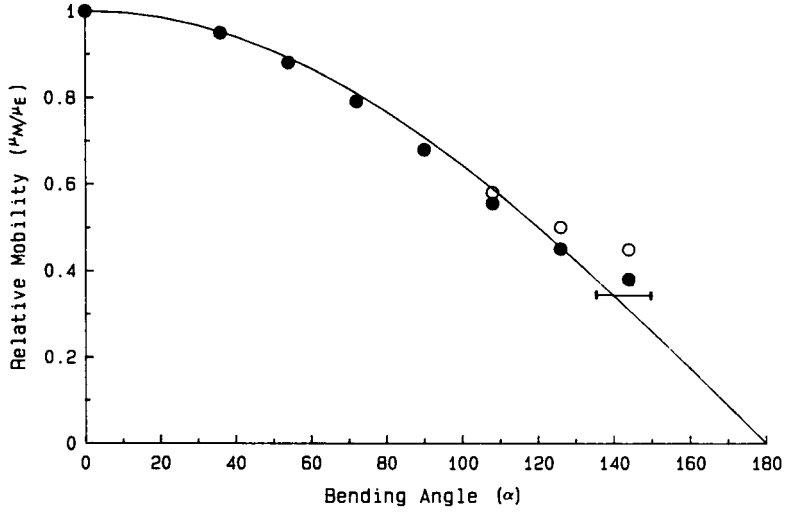

Fig. 5. Fitting of mobility data to a cosine function. The relative mobilities (μ_M/μ_E) of A tract DNA on 8% acrylamide gels is plotted versus predicted bending angle (α). The open circles represent actual mobilities while the closed circles have been corrected as described in the text to eliminate deviations caused by delocalization of the bend. The bar indicates the range of CAP bending angles predicted by electrostatic modeling (33). The solid line is cos $\alpha/2$.

acrylamide concentration and DNA length. Alteration of these conditions results in deviations from the equation. A different empirical equation relating curvature and mobility has been formulated for short DNA fragments that contain A tracts throughout their length (29), but these fragments are much shorter and more highly curved than those used here. The behavior of longer fragments that are curved throughout their length have also been modeled (34), but the A tracts studied here are not long enough to generate the superhelical configuration postulated in that model.

The validity of the above relation under these conditions can be tested by comparing the relative electrophoretic mobility with the calculated end-to-end distance for an entire set of protein-bound permuted fragments. The law of cosines was used to generate a relation for the end-to-end distance (h) of a DNA with a bend (α) cleaved at a fractional distance x from the end: $h^2=1-2x(1-\cos\alpha)+2x^2(1-\cos\alpha)$. When this relation is used with EcoRI, the calculated end-to-end distance and the observed mobility are proportional, irrespective of the position of the bend. However, with the sharply bent IHF-bound fragments, this is not observed, indicating that factors other than the end-to-end distance play an important role in their mobility.

Like CAP, the structure of EcoRI has been analyzed via crystallography, but the length of the oligomer in the co-crystal was not sufficient for a return to normal B structure beyond the protein-induced bends (35). The two deformations (type II neokinks) present in an EcoRI binding site each bend the DNA by 30° +/-10° and are located half a helical turn apart. Depending on how the bend is distributed between roll and tilt components, the bend could either cancel or add, respectively (36), for a total angle of up to 60° +/- 20°. This compares favorably with the values obtained for the three different EcoRI sites studied here (52°, 63°, 66°) (Table II). The value of 52° should be the most accurate because it was obtained with fragments that had no intrinsic curvature.

The degree of bending induced by proteins bound to sites in different sequence contexts has been examined with both EcoRI and IHF. For both proteins, there is relatively little variation

among the different sites examined (Table II). The effect of IHF binding has also been analyzed by others and found to produce extreme mobility shifts in all cases (37-39). EcoRI is not readily compared with similar enzymes because most restriction enzymes that we have tested are not amenable to the type of analysis performed here due to the lack of specific binding in the absence of magnesium (data not shown).

DISCUSSION

Role of bending in recombination

The behavior of Int bound to core-type sites must be viewed cautiously because of the relatively high non-specific affinity of Int for DNA (11). Int may slide between the weak core-type sites and non-specific sites as suggested by the affinity-dependent sliding of IHF between neighboring sites (37). Because there are so many potential non-specific sites and their effect is seen in aggregate in a mobility shift assay, the primary contribution to the observed mobility of DNA with core-bound Int may be from non-specific sites. However, these reservations do not apply to Int bound at the stronger arm-type sites that are readily distinguished from non-specific DNA via mobility shift assays.

The bending we have observed in the lambda recombination system appears to be required for the proper assembly of recombinogenic complexes rather than for rendering phosphodiester bonds more scissile. However, the possibility remains that core-bound Int can introduce transient bends into the DNA that facilitate strand cleavage. Int is able to specifically cleave att site DNA at high yields in the absence of IHF or supercoiling (40). In contrast, $\gamma\delta$ resolvase and the related Gin recombinase induce stable bends into their substrate DNAs near the sites of strand exchange (41,42).

The bending angles in Table II can be used to begin constructing models of att complexes. Because the IHF induced bends are the largest in magnitude and are also centrally placed, they will be the most significant determinants of the shape of the DNA within att complexes. Using CAP as the best available standard, we presently estimate the IHF-induced bend at greater

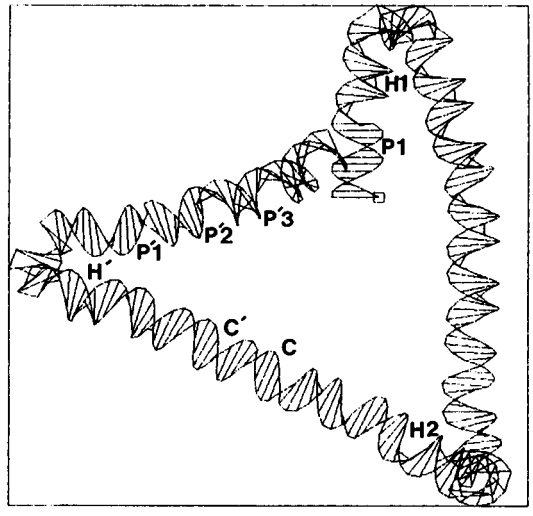

Fig. 6. One potential for the path of DNA in the attP complex. The bending angles in Table II were used with the DNA bending program from DNASTAR Inc. (Madison, WI) adapted from the helix trajectory program of Levene and Crothers (55). The Int and A tract bends were assigned arbitrary directions relative to IHF to allow depiction of the model. The IHF-induced bend was estimated at 160° from the equation in Fig. 5 but this value is uncertain until standards in this range can be obtained. The bend at each IHF site was evenly distributed at three positions separated by 5 bp. Int bends were placed at the center of each recognition sequence and A tract bends were split between the two junctions.

than 140°. Although the direction of the bends relative to each other has not yet been determined, an arbitrary phasing of A tract, IHF, and Int-induced bends can be assigned in order to visualize possible models for these complexes (Fig. 6). Since other looped structures can be generated with variations in these parameters, current models are only intended as a rough framework on which to incorporate accumulating biochemical data for these complex nucleoprotein structures.

Topological studies have shown that attP must make DNA loops around the core region to explain the catenated and knotted structures generated by integrative recombination (43-45). The models derived from bending data similarly predict loops with attP but, information about the phasing of bends will have to be obtained before it can be determined if the correct number and handedness of these loops can be predicted solely on the basis of

bending. The degree of DNA folding in this attP model provides possible mechanisms for long-range interactions detected by other techniques (9,14). In addition, the overall shape of the DNA in Fig. 6 shows a resemblance to the lobed attP "intasome" observed via electron microscopy (46). It should be noted that the bending measurements were done in the absence of supercoiling which is required for the formation of active complexes in integrative but not excisive recombination. Divalent cations are also required for recombination and will likely affect bending and/or protein-protein interactions.

Construction of models like that in Fig. 6 is based on the implicit assumption that the three-dimensional geometry of the nucleoprotein complex arises from bending of the DNA in localized regions and that the DNA is not uniformly wrapped around a multi-protein core with continuous protein-DNA contacts as might be expected in a nucleosome-like structure. This view is supported by studies of attP DNAs in which insertions and deletions of up to 20 bp were made adjacent to the required P1-H1 sites, changing their distance from the core (47). Integrative recombination was found to vary in a periodic fashion with efficient recombination occurring when the spacing changes placed the P1-H1 sites on the proper side of the DNA helix with respect to the core region. The relative independence of the reaction from absolute DNA length suggests that smooth wrapping does not occur.

Further characterization of the protein-induced bending of DNA in these complexes will be necessary to illuminate the structural properties important for executing site-specific recombination. The empirically-derived relation between bending angle and electrophoretic mobility affords a relatively simple technique for estimating bending angles that should be readily applicable to many systems where questions of higher-order structure are important for understanding function.

ACKNOWLEDGEMENTS

We thank the laboratories of R. Kahmann (Max Planck Institut, Berlin) and D. Crothers (Yale University) for generous gifts of FIS and CAP, respectively, and N. Cozzarelli, R. Kahmann, H. Nash, H. Nelson, J. Rosenberg, and T. Steitz for

communicating results prior to publication. Supported by American Cancer Society grant NP625 (J.T.) and NIH grants AI13544 and GM33928 (A.L.).

+Present address: Department of Molecular Genetics, Pfizer Central Research, Groton, CT 06340, USA

*To whom correspondence should be addressed

REFERENCES

1. Ptashne, M. (1986) Nature 322, 697-701.
2. Echols, H. (1986) Science 233, 1050-1056.
3. Richmond, T. J., Finch, J. T., Rushton, B., Rhodes, D. and Klug, A. (1984) Nature 311, 532-537.
4. Burlingame, R. W., Love, W. E., Wang, B. -C., Hamlin, R., Xuong, N. -H. and Moudrianakis, E. N. (1985) Science 228, 546-553.
5. Weisberg, R. A. and Landy, A. (1983) in Lambda II, Hendrix, R., Roberts, J., Stahl, F., Weisberg, R., eds. (Cold Spring Harbor Laboratory Press, Cold Spring Harbor, NY), p. 211-250.
6. Nash, H. A. (1981) Annu. Rev. Genet. 15, 143-167.
7. Bushman, W., Thompson, J. F., Vargas, L. and Landy, A. (1985) Science 230, 906-911.
8. Thompson, J. F., Waechter-Brulla, D., Gumport, R. I., Gardner, J. F., Moitoso de Vargas, L. and Landy, A. (1986) J. Bacteriol. 168, 1343-1351.
9. Thompson, J. F., Moitoso de Vargas, L., Skinner, S. E. and Landy, A. (1987) J. Mol. Biol. 195, 481-493.
10. Ross, W. and Landy, A. (1982) Proc. Natl. Acad. Sci. USA 79, 7724-7728.
11. Ross, W. and Landy, A. (1983) Cell 33, 261-272.
12. Craig, N. L. and Nash, H. A. (1984) Cell 39, 707-716.
13. Yin, S., Bushman, W. and Landy, A. (1985) Proc. Natl. Acad. Sci. USA 82, 1040-1044.
14. Richet, E., Abcarian, P. and Nash, H. A. (1986) Cell 46, 1011-1021.
15. Bauer, C. E., Hesse, S. D., Gumport, R. I. and Gardner, J. F. (1986) J. Mol. Biol. 192, 513-527.
16. Gardner, J. F. and Nash, H. A. (1986) J. Mol. Biol. 191, 181-189.
17. Thompson, J. F., Moitoso de Vargas, L., Koch, C., Kahmann, R. and Landy, A. (1987) Cell 50, 901-908.
18. Marini, J. C., Levene, S. D., Crothers, D. M. and Englund, P. T. (1982) Proc. Natl. Acad. Sci. USA 79, 7664-7668.
19. Hagerman, P. J. (1984) Proc. Natl. Acad. Sci. USA 81, 4632-4636.
20. Ulanovsky, L., Bodner, M., Trifonov, E. N. and Choder, M. (1986) Proc. Natl. Acad. Sci. USA 83, 862-866.
21. Levene, S. D., Wu, H. -M., and Crothers, D. M. (1986) Biochemistry 25, 3988-3995.
22. Griffith, J., Bleyman, M., Rouch, C. A., Kitchen, P. A. and Englund, P. T. (1986) Cell 46, 717-724.
23. Burkhoff, A. M. and Tullius, T. D. (1987) Cell 48, 935-943.
24. Zahn, K. and Blattner, F. R. (1987) Science 236, 416-422.
25. Nelson, H. C. M., Finch, J. T., Luisi, B. F. and Klug, A. (1987) Nature 330, 221-226.

26. Wu, H. -M. and Crothers, D. M. (1984) Nature 308, 509-513.
27. Diekmann, S. and Wang, J. C. (1985) J. Mol. Biol. 186, 1-11.
28. Koo, H. -S., Wu, H. -M. and Crothers, D. M. (1986) Nature 320, 501-506.
29. Koo, H. -S. and Crothers, D. M. (1988) Proc. Natl. Acad. Sci. USA 85, 1763-1767.
30. Lumpkin, O. J., Dejardin, P. and Zimm, B. H. (1985) Biopolymers 24, 1573-1593.
31. Southern, E. M. (1979) Anal. Biochem. 100, 319-323.
32. Stellwagen, N. C. (1983) Biochemistry 22, 6186-6193.
33. Warwicker, J., Engelman, B. P. and Steitz, T. A. (1987) Proteins 2, 283-289.
34. Calladine, C. R., Drew, H. R. and McCall, M. J. (1988) J. Mol. Biol. 201, 127-137.
35. McClarin, J. A., Frederick, C. A., Wang, B. -C., Greene, P., Boyer, H. W., Grable, J. and Rosenberg, J. M. (1986) Science 234, 1526-1541.
36. Ulanovsky, L. E. and Trifonov, E. N. (1987) Nature 326, 720-722.
37. Prentki, P., Chandler, M. and Galas, D. J. (1987) EMBO J. 6, 2479-2487.
38. Stenzel, T. T., Patel, P. and Bastia, D. (1987) Cell 49, 709-717.
39. Robertson, C. A. and Nash, H. A. (1988) J. Biol. Chem. 263, 3554-3557.
40. Pargellis, C. A., Nunes-Duby, S. E., Moitoso de Vargas, L. and Landy, A. (1988) J. Biol. Chem. 263, 7678-7685.
41. Hatfull, G. F., Noble, S. M. and Grindley, N. D. F. (1987) Cell 49, 103-110.
42. Mertens, G., Klippel, A., Fuss, H., Blocker, H., Frank, R. and Kahmann, R. (1988) in press.
43. Pollock, T.J. and Nash, H.A. (1983) J. Mol. Biol. 170, 1-18.
44. Griffith, F. D. and Nash, H. A. (1985) Proc. Natl. Acad. Sci. USA 82, 3124-3128.
45. Spengler, S. J., Stasiak, A. and Cozzarelli, N. R. (1985) Cell 42, 325-334.
46. Better, M., Lu, C., Williams, R. C. and Echols, H. (1982) Proc. Natl. Acad. Sci. USA 79, 5837-5841.
47. Thompson, J. F., Snyder, U. K. and Landy, A. (1988) Proc. Natl. Acad. Sci., USA 85, 000-000.
48. Thompson, J. F., Mark, H. F. L., Franz, B. and Landy, A. (1988) in DNA Bending and Curvature, Olson, W. K., Sarma, M. H., Sarma, R. H. and Sundaralingam, M., eds. (Adenine Press, Guilderland, NY), p. 119-128.
49. Messing, J. (1983) Meth. Enzymology 101, 20-78.
50. Nash, H. A. (1975) Proc. Natl. Acad. Sci. USA 72, 1072-1076.
51. Nash, H. A. and Robertson, C. A. (1981) J. Biol. Chem. 256, 9245-9253.
52. Abremski, K. and Gottesman, S. (1982) J. Biol. Chem. 257, 9658-9662.
53. Shuey, D. J. and Parker, C. S. (1986) Nature 323, 459-461.
54. Liu-Johnson, H. N., Gartenberg, M. R. and Crothers, D. M. (1986) Cell 47, 995-1005.
55. Levene, S. D. and Crothers, D. M. (1983) J. Biomol. Stereodynamics 1, 429-435.
56. Bushman, W., Yin, S., Thio, L.-L. and Landy, A. (1984) Cell 39, 699-706.